DET NORSKE VERITAS

Final Report
Compatibility of Non-Ferrous Metals with Fuel Grade Ethanol

Pipeline & Hazardous Materials Safety Administration
U.S. Department of Transportation

Report No./DNV Reg No.: ANEUS811GUI (EP021140)
March 14, 2011

Compatibility of Non-Ferrous Metals with Ethanol	DET NORSKE VERITAS (U.S.A.), INC. Materials & Corrosion Technology Center 5777 Frantz Road Dublin, OH 43017-1386, United States Tel: (614) 761-1214 Fax: (614) 761-1633 http://www.dnv.com http://www.dnvcolumbus.com
For: Pipeline & Hazardous Materials Safety Administration U.S. Department of Transportation East Building, 2nd Floor 1200 New Jersey Ave., SE Washington, DC 20590	
Account Ref.:	

Date of First Issue:	March 14, 2011	Project No.	EP021140
Report No.:		Organization Unit:	Materials & Corrosion Technology Ctr.
Revision No.:	0	Subject Group:	
Summary:			
See Executive Summary			

Prepared by:	Feng Gui	*Signature*
Verified by:	John Beavers	*Signature*
Approved by:	Oliver Moghissi	*Signature*

☑	No distribution without permission from the client or responsible organizational unit (however, free distribution for internal use within DNV after 3 years)	Indexing Terms	
☐	No distribution without permission from the client or responsible organizational unit	Key Words	
☐	Strictly confidential	Service Area	
☐	Unrestricted distribution	Market Segment	

Rev. No. / Date:	Reason for Issue:	Prepared by:	Approved by:	Verified by

© 2011 Det Norske Veritas (U.S.A.), Inc.
All rights reserved. This publication or parts thereof may not be reproduced or transmitted in any form or by any means, including photocopying or recording, without the prior written consent of Det Norske Veritas (U.S.A.), Inc.

Executive Summary

Ethanol has attracted much attention in recent years as an alternative fuel source in an effort to improve security of supply and energy independence. In the US, the Energy Independence and Security Act of 2007 calls for consumption of 36 billion gallons of alternate fuels, including ethanol, per year by 2022. Worldwide, ethanol demand is expected to more than double in the next ten years. Although most of the ethanol is currently transported by tanker trucks, rail cars, and barges, pipelines are still the most efficient system to transport ethanol. Thus, with increases in ethanol demand, it is expected that pipelines, both existing pipeline infrastructure and new pipelines, will play a major role in transporting ethanol.

The vast majority of research related to materials compatibility with ethanol transportation has been performed with carbon steels (tank and pipeline steels), but a few references to non-ferrous materials compatibility can be found in the literature dating back to before World War II.

The primary objective of the proposed work is to provide an improved understanding of the performance of non-ferrous metals and stainless steels in fuel grade ethanol (FGE). To achieve the project objective, two technical tasks were conducted; (1) a state-of-the-art survey was conducted on compatibility issues with the most common non-ferrous metals found in pipeline systems, terminals, and other down-stream components in the supply chain, and (2) laboratory testing was performed to evaluate the performance of a selected set of non-ferrous metals where limited or no service record is available. The project was primarily focused on non-ferrous metals found in pipeline systems, terminals, and downstream components in the supply chain. The state-of-the-art survey task was cosponsored by PRCI and PHMSA and was completed in PRCI Project PR-186-09204. A report was submitted to PRCI in 2010.

Key Results of the PRCI Project

The materials compatibility data were divided into four different categorizations. *Not Compatible* indicates that sufficient information was found to establish that the class of materials is not compatible. *Probably Not Compatible* indicates that information was limited but the available information suggests that the class of materials is not compatible. *Probably Compatible* indicates that information was limited but the available information suggests that the class of materials is compatible. *Compatible* indicates that sufficient information was found to establish that the class of materials is compatible.

Zinc and aluminum are not compatible metallic materials in ethanol. Aluminum has exhibited pitting and SCC in ethanol, while zinc has exhibited high rates of general corrosion, pitting, and intergranular attack in ethanol. Titanium is probably not compatible, as it has been reported to be susceptible to SCC in ethanol. With the exception of brasses and other copper alloys that contain significant concentrations of zinc, copper base alloys, nickel base alloys, and stainless steels are probably compatible in ethanol, but more testing is needed on SCC behavior given the

limited information on this failure mode and the SCC experience with carbon steels. There was insufficient information in the literature to confirm the compatibility of any metallic materials.

The following materials were selected for laboratory evaluation based on the PRCI report:

- Bronze 10%;
- Brass 70-30;
- Nickel Alloy 200;
- Stainless Steel 304;
- Stainless Steel 316;
- Aluminum Alloy 7075

Key Results of the Laboratory Testing:

- AA7075, Bronze 10% and Nickel Alloy were found to be susceptible to pitting corrosion in the laboratory tests. AA7075 had a repassivation potential below the open circuit potential (OCP) in aerated E95, indicating a high likelihood of pitting corrosion. Bronze 10% also had a repassivation close to the OCP in the aerated E95, meaning the likelihood of pitting corrosion is higher than other tested materials.

- The materials did not show a substantial difference in the corrosion performance in E50 and E95.

- The general corrosion rates, in general, were very low for all materials in all tested solutions.

- The general corrosion rate of Bronze 10% was the highest among all tested materials independent of tested solutions and the purging gas but was low from the standpoint of material integrity.

- The addition of 37.5 ppm NH_4OH did not substantially alter the material corrosion performance of the tested materials. An increase in the anodic current was noted for Bronze 10% in E95 in the presence of 37.5 ppm NH_4OH but the corrosion rate was still minimal.

Table of Contents

1.0 BACKGROUND 1

2.0 PROJECT OBJECTIVE 2

3.0 RESULTS 3

3.1 Task 1: State of the Art Survey on Compatibility Issues with Non-Ferrous Metals 3

3.1.1 Technical Approach 3

3.1.2 Key Results 3

3.2 Task 2: Laboratory Testing of Non-Ferrous Metals in FGE 4

3.2.1 Experimental Approach 4

3.2.2 Results in E95 9

3.2.3 Results in E50 18

3.2.4 Results in E95 with 37.5 ppm NH_4OH 24

4.0 GENERAL DISCUSSION 28

5.0 SUMMARY 29

6.0 REFERENCES 29

List of Tables

Table 1. Metals Compatible with low and high concentration ethanol fuels [7]. 2

Table 2. Chemical composition of the tested materials. 5

Table 3. Test matrix. 5

Table 4. Target composition of SFGE. 6

Table 5. OCP and critical pitting potential (E_{Pit}) and repassivation potential (E_{rp}) for the materials tested in E95 15

Table 6. Corrosion rates (mpy) of the materials tested in E95. 17

Table 7. Comparison of OCP, critical pitting potential (E_{Pit}) and the repassivation potential (E_{rp}) for the materials tested in E50 (unit: V vs. Ag/AgCl). 22

Table 8. Corrosion rate (mpy) of non-ferrous materials in E50 24

Table 9. Corrosion rate (mpy) of non-ferrous materials in deaerated E95 with 37.5 ppm NH_4OH..... 28

List of Figures

Figure 1. Illustrations of the electrochemical experimental setup (a) and the test cell (b). 8

Figure 2. A schematic cyclic potentiodynamic polarization (CPP) curve. 8

Figure 3. Comparison of CPP curves obtained for AA7075 in E95 at different aeration conditions. 9

Figure 4. Optical photographs of the AA7075 samples tested in E95 under (a) aerated condition and (b) deaerated condition 10

Figure 5. Comparison of CPP curves obtained for brass in E95 at different aeration conditions. 10

Figure 6. Optical photographs of the brass samples tested in E95 under (a) aerated condition and (b) deaerated condition. 11

Figure 7. Comparison of CPP curves obtained for bronze in E95 at different aeration conditions. 11

Figure 8. Optical photographs of the bronze samples tested in E95 under (a) aerated condition and (b) deaerated condition. 12

Figure 9. Comparison of CPP curves obtained for Nickel Alloy 200 in E95 at different aeration conditions. 12

Figure 10. Optical photographs of the Nickel Alloy 200 samples tested in E95 under (a) aerated condition and (b) deaerated condition. 13

Figure 11. Comparison of CPP curves obtained for SS304 in E95 at different aeration conditions. 13

Figure 12. Optical photographs of the SS304 samples tested in E95 under (a) aerated condition and (b) deaerated condition. 14

Figure 13. Comparison of CPP curves obtained for SS316 in E95 at different aeration conditions. 14

Figure 14. Optical photographs of the SS316 samples tested in E95 under (a) aerated condition and (b) deaerated condition. 15

Figure 15. Comparison of the OCP, pitting potential and the repassivation potential for different tested materials in SFGE under deaerated aerated conditions (a) and deaerated conditions (b). 16

Figure 16. Comparison of the corrosion rates of the tested materials in SFGE. 17

Figure 17. Comparison of CPP curves obtained for AA7075 in E50 at different aeration conditions. 18

Figure 18. Optical photographs of the AA7075 samples tested in E50 under (a) aerated condition and (b) deaerated condition. 19

Figure 19. Comparison of CPP curves obtained for Bronze in E50 at different aeration conditions. 19

Figure 20. Optical photographs of the Bronze samples tested in E50 under (a) aerated condition and (b) deaerated condition. 20

Figure 21. Comparison of CPP curves obtained for Nickel Alloy 200 in E50 at different aeration conditions. 20

Figure 22. Optical photographs of the Nickel Alloy 200 samples tested in E50 under (a) aerated condition and (b) deaerated condition. 21

Figure 23. Comparison of CPP curves obtained for Nickel Alloy 200 in E50 at different aeration conditions. 21

Figure 24. Optical photographs of the Nickel Alloy 200 samples tested in E50 under (a) aerated condition and (b) deaerated condition. 22

Figure 25. Comparison of OCP, pitting potential and repassivation potential for different tested materials in E50 under deaerated aerated conditions (a) and deaerated conditions (b). 23

Figure 26. Comparison of corrosion rates of the tested materials in SFGE. 24

Figure 27. Comparison of CPP curves obtained for AA7075 in deaerated E95 with 37.5 ppm NH_4OH. 25

Figure 28. Optical photographs of the AA7075 samples tested in deaerated E50. (a) with 37.5 ppm NH_4OH; (b) without NH_4OH. 25

Figure 29. Comparison of CPP curves obtained for Bronze in deaerated E95 with 37.5 ppm NH_4OH. 26

Figure 30. Optical photographs of the Bronze samples tested in deaerated E50. (a) with 37.5 ppm NH_4OH; (b) without NH_4OH. 26

Figure 31. Comparison of CPP curves obtained for Nickel Alloy 200 in deaerated E95 with 37.5 ppm NH_4OH. 27

Figure 32. Optical photographs of the Nickel Alloy 200 samples tested in deaerated E50. (a) with 37.5 ppm NH_4OH; (b) without NH_4OH. 27

Figure 33. Comparison of corrosion rates of the tested materials in deaerated E95 with and without 37.5 ppm NH_4OH. 28

1.0 BACKGROUND

Ethanol has attracted much attention in recent years as an alternative fuel source in an effort to improve security of supply and energy independence. In the US, the Energy Independence and Security Act of 2007 calls for a consumption of 36 billion gallons of alternate fuels, including ethanol, per year by 2022. Worldwide, ethanol demand is expected to more than double in the next ten years. Although most of the ethanol is currently transported by tanker trucks, rail cars, and barges, pipelines are still the most efficient system to transport ethanol. Thus, with increases in ethanol demand, it is expected that pipelines, both existing pipeline infrastructure and new pipelines, will play a major role in transporting ethanol.

Several materials compatibility issues must be resolved before fuel grade ethanol (FGE) can be transported in pipelines. These issues include stress corrosion cracking (SCC), corrosion, elastomer compatibility, and monitoring. While SCC of pipeline steels is probably the most significant unresolved technical issue, the compatibility of non-ferrous metals and stainless steels found in most pipeline systems also is an area of concern. Non-ferrous metals also are found in distribution terminals, service stations, and in automobiles. In the Roadmapping Workshop, conducted in October 2007, an understanding of how existing materials and new materials are affected by FGE was identified as a major gap in the safe transportation of ethanol in pipelines.

While technical gaps remain unresolved, API, RFA, PRCI, and PHMSA, have funded a significant amount of research to address the major technical gaps associated with ferrous metals such as the pipeline steels. On the other hand, very little research has been done to address the issue of compatibility of non-ferrous metals and stainless steels with FGE.

The vast majority of research related to materials compatibility with ethanol transportation has been performed with ferrous metals, but a few references to non-ferrous materials compatibility can be found in the literature dating back to before World War II. Evans [2], in 1948, stated that "The use of ethyl alcohol as a fuel lends interest to its action on metals – a matter investigated by Gindin [2] and his colleagues." Gindin reported that magnesium was found to be slightly attacked by alcohol, whereas aluminum, zinc, and steel were relatively resistant. Gindin also reported that several inhibitors, including paraldehyde and benzaldehyde, were effective in reducing the extent of attack of all three metals. Bushrod [3] reported that small additions of ammonium oleate to methyl and ethyl alcohols (used as cooling agents in aircraft) were effective in reducing corrosion of magnesium alloys. Almost all these alloys tested are probably non-existent today, essentially rendering these data to be of only historical importance.

API Technical Report 939-D [4] summarized the results of a literature search performed on corrosion and SCC in alcohol containing environments. References are discussed relating to SCC of titanium in methanolic environments and zirconium in several alcohols including

ethanol. In the latter research, intergranular SCC of zirconium was reported, and the severity of cracking decreased with increasing chain length of the alcohol [5]. API Technical Report 939-D [4] also contains a very limited discussion of the literature on the compatibility of stainless steels in alcohols. Singh [6] reported that pitting of Type 321 stainless steel was extensive in ethanol solutions containing sulfuric acid, whereas, pitting was not observed in isopropanol and butanol solutions containing similar sulfuric acid concentrations. API Technical Report 939-D [4] contains no references to the compatibility of other common materials, such as aluminum and copper alloys, in ethanolic solutions.

The Renewable Fuels Association (RFA) has issued brief guidelines for metals compatibility in ethanolic fuels [7]. These guidelines are summarized in Table 1. Note that mild steel is considered acceptable for use in E85, in spite of the fact that this material has demonstrated susceptibility to SCC in ethanol-gasoline blends. This suggests that not all of the corrosion related issues for these metals have been fully addressed.

Table 1. Metals Compatible with low and high concentration ethanol fuels [7].

Metals Compatibility Issues in **E10** Fuels		Metals Compatibility Issues in **E85** Fuels	
Recommended	Not Recommended	Recommended	Not Recommended
Aluminum Black iron Brass Bronze Carbon steel Stainless steel	Galvanized zinc	Bronze Black iron Mild steel Stainless steel Unplated steel Nickel-plated aluminum or brass Aluminum alloy	Brass Lead Lead solder Magnesium Lead-tin alloy (tin-plated steel) Zinc

In summary, research on the compatibility of non-ferrous metals with ethanol has been conducted for more than sixty years but the work has been limited in scope and a comprehensive assessment of this issue has not been performed.

2.0 PROJECT OBJECTIVE

The primary objective of the proposed work is to provide an improved understanding on the performance of non-ferrous metals and stainless steels in FGE. To achieve the project objective, two technical tasks were conducted; (1) a state-of-the-art survey was conducted on compatibility issues with the most common non-ferrous metals found in pipeline systems, terminals, and other down-stream components in the supply chain, and (2) laboratory testing was performed to evaluate the performance of a selected set of non-ferrous metals where limited or no service

record is available. The project was primarily focused on non-ferrous metals found in pipeline systems, terminals, and downstream components in the supply chain. The state-of-the-art survey task was cosponsored by PRCI and PHMSA and was completed in PRCI Project PR-186-09204 [8]. A report was submitted to PRCI in 2010. The materials tested in this project in Task 2 were based on the knowledge gained in the PRCI project.

3.0 RESULTS

3.1 Task 1: State of the Art Survey on Compatibility Issues with Non-Ferrous Metals

This task was completed in PRCI Project PR-186-09024. The technical approach and the key findings are summarized below.

3.1.1 Technical Approach

The first task in Phase 1 of this project involved sending out an industry survey regarding materials in pump stations. This task was performed to determine what components are important from a facilities point of view and what materials are used in these components. The information from the survey was organized into a table that is attached as an appendix to this report. Additionally, manufacturers of the components were contacted in order to determine the materials present in the components in the pump stations. The requests for bill of materials or materials for specific part numbers were performed by email and/or phone calls.

The second task involved performing a literature search. The survey focused on data from the literature on the ethanol exposure effects of materials involved in various pump station components. The open literature and company reports were considered. Previous literature surveys conducted for PRCI SCC 4-1 and 4-4, and API, were utilized. The open literature search was performed using two search engines; Engineering Village and Science Direct. The keywords in the search included ethanol, corrosion, failure, various non-ferrous metals, stainless steels, and elastomers/plastics.

3.1.2 Key Results

A number of different materials were found to be present in the components in pump stations. Metals included carbon and low alloy steels, stainless steels, pure nickel, bronzes, and aluminum alloys. There was a variety of stainless steels in pump station components including 300 series (austenitic, high nickel), 400 series (ferritic/martensitic, low nickel) and precipitation hardened alloys. Zinc and titanium were included in the literature search results; although they were not

identified in pump station equipment. Non-metallic materials in pump station components include ceramics, fiberglass, Buna N and butadiene rubbers, polyurethane, Teflon, PEEK, Viton®, and nylon.

No information was found on the performance of ceramic materials in ethanol and the literature on the performance of metallic materials in ethanol is relatively limited. More information was found on elastomer compatibility in ethanol. Information on compatibility in actual FGE was generally more limited than that in other ethanolic solutions.

The materials compatibility data were divided into four different categorizations. *Not Compatible* indicates that sufficient information was found to establish that the class of materials is not compatible. *Probably Not Compatible* indicates that information was limited but the available information suggests that the class of materials is not compatible. *Probably Compatible* indicates that information was limited but the available information suggests that the class of materials is compatible. *Compatible* indicates that sufficient information was found to establish that the class of materials is compatible.

Zinc and aluminum are not compatible metallic materials in ethanol. Aluminum has exhibited pitting and SCC in ethanol, while zinc has exhibited high rates of general corrosion, pitting, and intergranular attack in ethanol. Titanium is probably not compatible, as it has been reported to be susceptible to SCC in ethanol. With the exception of brasses and other copper alloys that contain significant concentrations of zinc, copper base alloys, nickel base alloys, and stainless steels are probably compatible in ethanol, but more testing is needed on SCC behavior given the limited information on this failure mode and the SCC experience with carbon steels. There was insufficient information in the literature to confirm the compatibility of any metallic materials.

3.2 Task 2: Laboratory Testing of Non-Ferrous Metals in FGE

3.2.1 Experimental Approach

Table 2 is the chemical composition nof the tested materials and Table 3 shows the test matrix. The tested materials were selected based on the finding in the PRCI survey summarized above in task 1 and the available budget for this project. It was recommended in the PRCI report that although some data are available for these materials, their susceptibility to pitting corrosion is unknown. Additionally, the available corrosion rate data were often not obtained in FGE. Therefore, these materials were tested to evaluate their susceptibility to pitting corrosion and also to obtain their corrosion rates in FGE solutions. Stainless steels (SS) 304 and 316 were also evaluated in addition to non-ferrous metals due to their wide usage in the pump stations. It should be noted that not every material identified in the PRCI project was tested due to the limitations on the available resource.

It was found in a previous research that oxygen is essential to maintain the passivity of carbon steel in SFGE. Thus, the materials were evaluated in FGE solutions under both deaerated (nitrogen purging) and aerated conditions (zero air purging) in most cases. The materials were also evaluated in E50 due to the finding that carbon steel was more susceptible to SCC in E50 than in E95 in the previous PHMSA funded studies. The compatibility of these materials was also investigated in the presence of NH_4OH. It has been demonstrated that NH_4OH was very effective in mitigating SCC of carbon steel in FGE [9]. The compatibility of the selected materials with FGE in the presence of NH_4OH (37.5 ppm) was evaluated.

Table 2. Chemical composition of the tested materials.

	Bronze 10%	Brass 70-30	Nickel Alloy 200*	Stainless steel 304	Stainless steel 316	Aluminum 7075
Iron	0.0054	0.02	0.01	-	-	0.5
Copper	87.973	70.19	<0.01	-	0.2	1.6
Lead	-	0.02	-	-	-	
Zinc	-	29.77	-	-	-	5.6
Tin	12	-	-	-	-	
Calcium	0.001	-	-	-	-	
Magnesium	0.0024	-	-	-	-	2.5
Manganese	0.001	-	0.2	1.4221	1.36	0.3
Nickel	0.003	-	99.67	8.4868	12.01	
Silicon	0.001	-	0.07	0.4542	0.38	0.4
Silver	0.013	-	-	-	-	
Carbon	-	-	0.05	0.0545	0.02	
Cobalt	-	-	<0.01	-	-	
Sulfur	-	-	0.001	0.001	0.001	
Chromium	-	-	-	18.261	17.27	0.26
Phosphorus	-	-	-	0.0296	0.025	
Nitrogen	-	-	-	0.738	0.035	
Molybdenum	-	-	-	-	2.06	
Zirconium	-	-	-	-	-	0.25
Titanium	-	-	-	-	-	0.2
Aluminum	-	-	-	-	-	88.39

Table 3. Test matrix.

Environment	Material					
	Brass (70-30)	Bronze (10% Sn)	Nickel 200	AA7075	Stainless Steel 316	Stainless Steel 304
E95 (Zero Air)	√	√	√	√	√	√
E95 (Nitrogen)	√	√	√	√	√	√
E50 (Zero Air)		√	√	√		√
E50 (Nitrogen)		√	√	√		√
E95 (Zero Air+NH_4OH)		√	√	√		

The electrochemical tests in FGE were performed using a technique developed to overcome the potential drop imposed by the resistance nature of the FGE solution [10]. The polarization scans were conducted in simulated FGE (SFGE). The SFGE was prepared with 200-proof ethanol and contaminants and additions found in the ASTM standard D4806 [11] with the composition listed in Table 4. The SFGE prepared following this procedure is referred as E95 in this report. The SFGE was also diluted with gasoline to obtained E50.

Table 4. Target composition of SFGE.

Requirement	ASTM Limits	
	Min.	Max.
Ethanol, vol. %	92.1	–
Methanol, vol. %	–	0.5
Solvent-washed gum, mg/100 ml	–	5.0
Water content, vol. %	–	1.0
Denaturant content, vol. %	1.96	5.00
Inorganic chloride, ppm (mg/L)	–	5
Copper, mg/kg	–	0.1
Acidity (as Acetic Acid CH_3COOH), mass % (mg/L)	–	0.007 (56)
pH_e	6.5	9.0

The samples were all 100 µm wires (California Fine Wires*). They were prepared by mounting a wire in the epoxy (electrode surface area 0.002 cm^2). A special two parts epoxy (EPON Resin 828 and EPIKURE 3234 curing agent†) was used owing to its extraordinary stability in organic solvents as demonstrated by others [12]. The mounted electrodes were left in air for a few days to fully cure. They were subsequently polished with 800 grit sand paper prior to being used in the experiments. An Ag/AgCl wire was used as the reference electrode and a Pt wire was used as the counter electrode. The AgCl film on the reference electrode was prepared by galvanostatically polarizing an Ag wire in 1 M HCl for 30 mins at a current density of 0.1 mA/cm^2. The reference electrode was positioned only a few millimeters away from the working electrode and the counter electrode was within 2 cm from the working electrode. The electrochemical experimental setup and the test cell used in this work are illustrated in Figure 1. Potentiodynamic polarization scans were performed on the microelectrodes using a VMP3 multichannel

* California Fine Wire Company, Grover Beach, CA
† Miller-Stephenson, IL, USA

potentiostat (Bio-Logic)*. The open circuit potential (OCP) was monitored for one hour in each test prior to the potentiodynamic scan. The cyclic potentiodynamic polarization (CPP) scans were conducted from -100 mV vs. OCP to 0.5 V vs. Ag/AgCl at a rate of 0.17 mV/s. The scan then was reversed at 0.5 V vs. Ag/AgCl and stopped at the OCP. The cells were placed inside a faraday cage to reduce the noise during the measurement. Upon completion of the potentiodynamic scan, the working electrode was inspected under an optical microscope.

Corrosion rates were obtained from the corrosion current density using the equations below:

$$CR = K_1 \frac{i_{corr}}{\rho} EW \qquad (1)$$

Where CR-- Corrosion rate (mpy)
K1- 0.1288 mpy g/μA cm
EW- equivalent weight of carbon steel
i_{corr}- corrosion current (μA/cm^2)
ρ – density (g/cm^3)

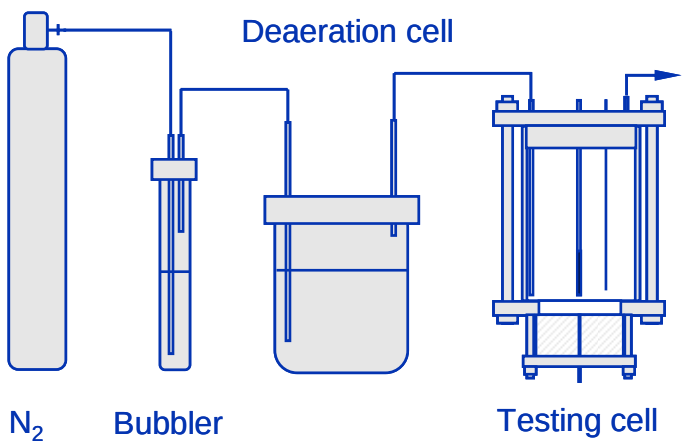

(a) experimental setup.

* Bio-Logic, France

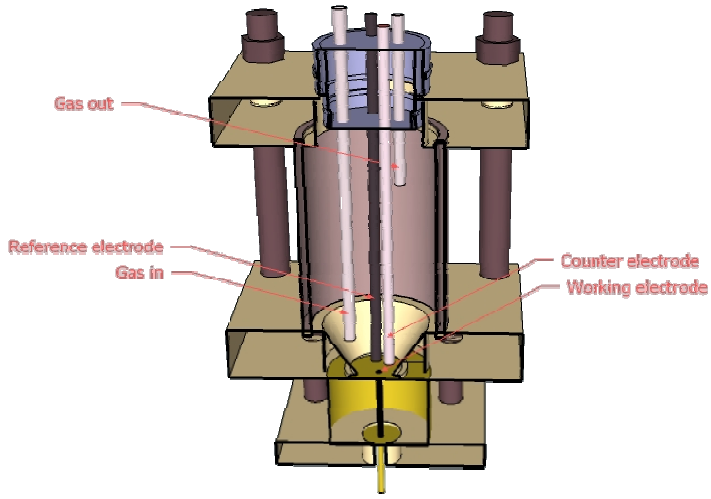

(b) test cell

Figure 1. Illustrations of the electrochemical experimental setup (a) and the test cell (b).

An example CPP curve is shown in Figure 2. Through the CPP testing, pitting potential (Epit) and repassivation potential (Erp) are obtained. The pitting potential is the potential above which the stable pitting corrosion would occur whereas the repassivation potential is the potential below which the material is immune to pitting corrosion.

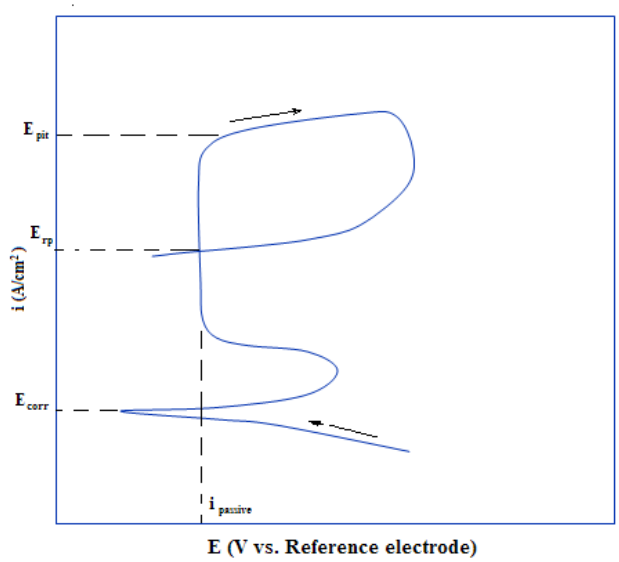

Figure 2. A schematic cyclic potentiodynamic polarization (CPP) curve.

3.2.2 Results in E95

As mentioned above, the CPP curves were obtained for all tested materials in E95 under both aerated and deaerated conditions. The pitting potentials were then obtained from the CPP curves and the corrosion rates were calculated using the equation listed above. These parameters were used to evaluate and compare the compatibility of various materials in E95.

Aluminum 7075 (AA7075)

The CPP curves of AA7075 obtained in E95 under aerated and deaerated conditions are compared in Figure 3. The passive current density for AA7075 appeared to be independent of the purging gas, which is different from carbon steel that showed lower passive current density in the presence of oxygen. As expected, the corrosion potential was more noble in the presence of oxygen compared to when the solution was purged with nitrogen (-0.625 V vs. -0.834 V vs. Ag/AgCl). Pitting corrosion was observed after the CPP tests, as shown in Figure 4, with the difference of the pitting potential and the OCP larger than 600 mV. The repassivation potential, however, was only 100 mV more positive than the OCP in the deaerated conditions and below the OCP in the aerated solution.

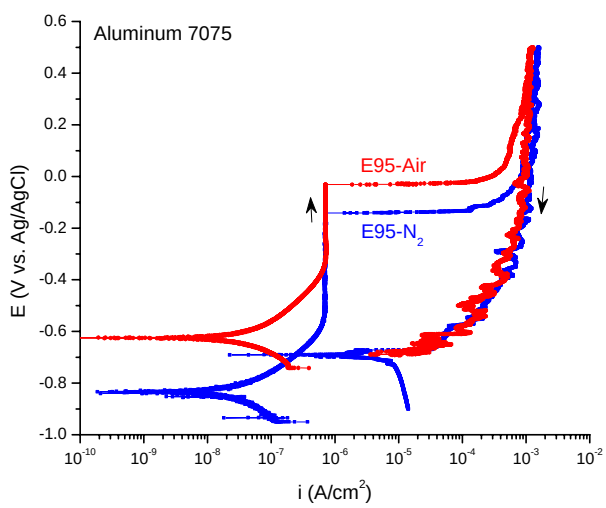

Figure 3. Comparison of CPP curves obtained for AA7075 in E95 at different aeration conditions.

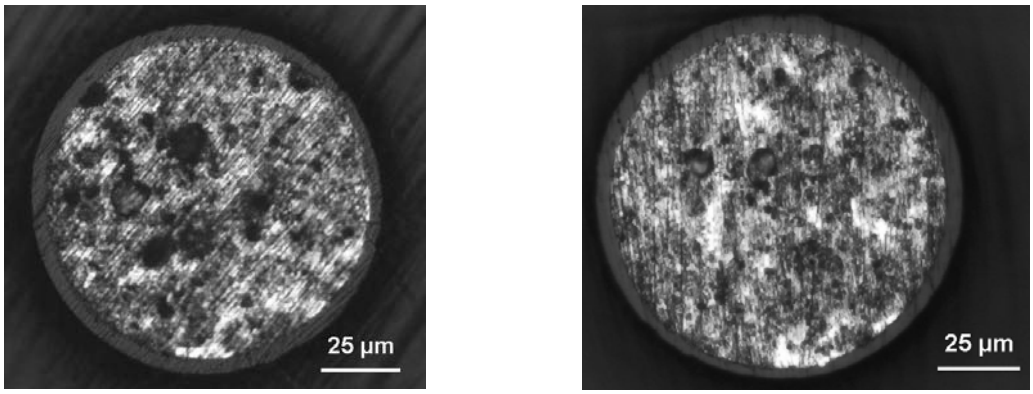

(a) (b)

Figure 4. Optical photographs of the AA7075 samples tested in E95 under (a) aerated condition and (b) deaerated condition

Brass 70-30

The CPP curves for Brass obtained in SFGE under aerated and deaerated conditions are compared in Figure 5. The samples experienced active corrosion at potentials slightly higher than OCP with and without oxygen. Similar to AA7075, the OCP of Brass was slightly more positive when the solution was purged by oxygen than by nitrogen. The general corrosion was confirmed by visually inspecting the samples after CPP tests, as shown in Figure 6.

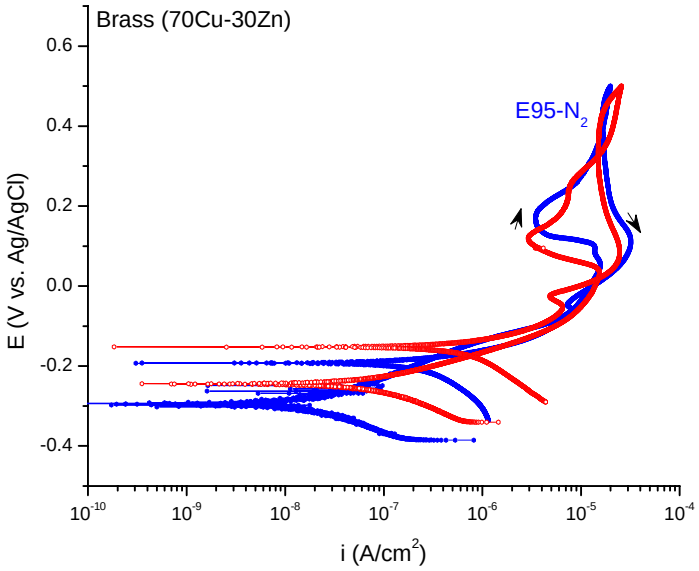

Figure 5. Comparison of CPP curves obtained for brass in E95 at different aeration conditions.

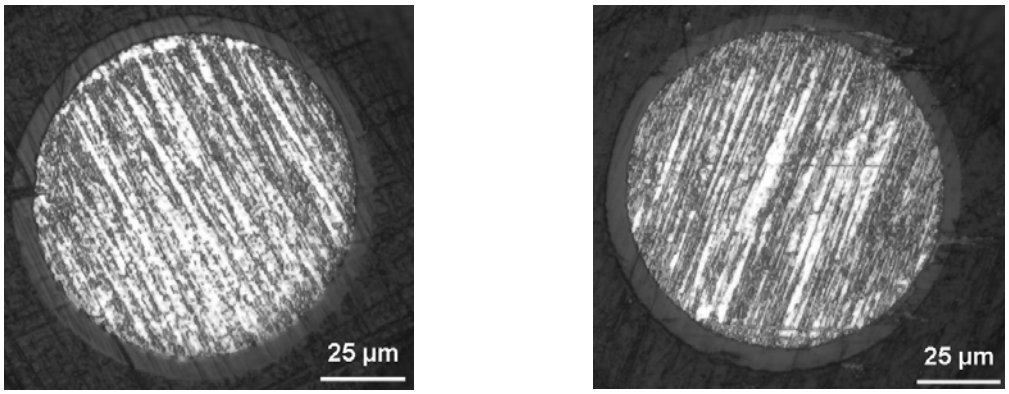

(a) (b)

Figure 6. Optical photographs of the brass samples tested in E95 under (a) aerated condition and (b) deaerated condition

Bronze 10%

The CPP curves for Bronze obtained in E95 under aerated and deaerated conditions are compared in Figure 7. Pitting corrosion was observed only when oxygen was present, as shown in Figure 8 (a). The pitting potential is approximately 0.2 V vs. Ag/AgCl and the repassivation potential is 0 V vs. Ag/AgCl, 100 mV more positive than the OCP. The OCP was moved from -0.193 V vs. Ag/AgCl to -0.096 V vs. Ag/AgCl in the presence of oxygen after one hour exposure.

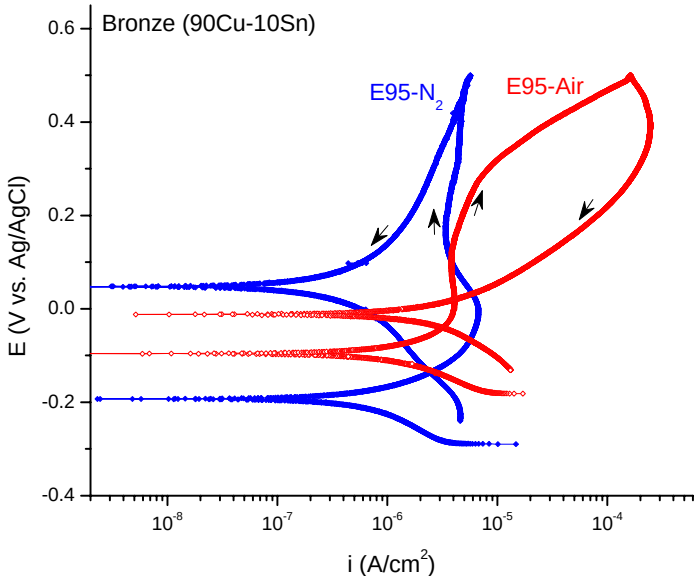

Figure 7. Comparison of CPP curves obtained for bronze in E95 at different aeration conditions.

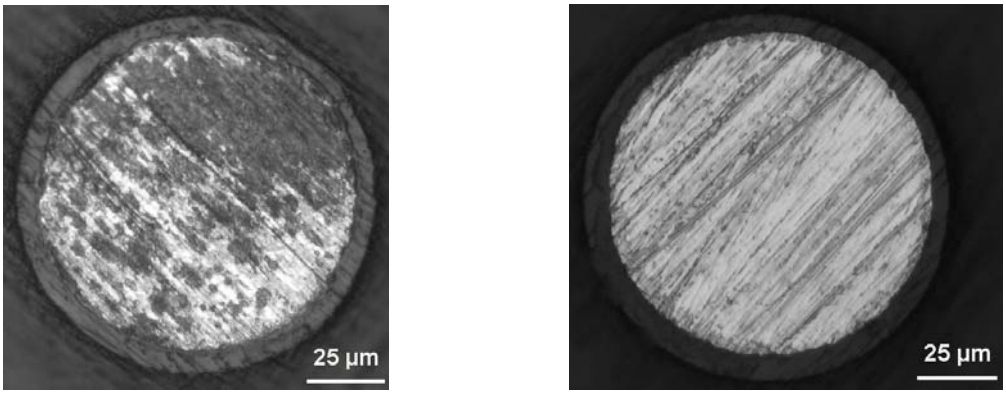

(a) (b)

Figure 8. Optical photographs of the bronze samples tested in E95 under (a) aerated condition and (b) deaerated condition.

Nickel alloy 200

The CPP curves for Nickel Alloy 200 obtained in E95 under aerated and deaerated conditions are compared in Figure 9. Pitting corrosion was observed in the presence of oxygen while the sample did not show any attack in deaerated E95 (Figure 10). The pitting potential was around +0.367 V vs. Ag/AgCl, 600 mV higher than the OCP and the repassivation potential is about 0 V vs. Ag/AgCl.

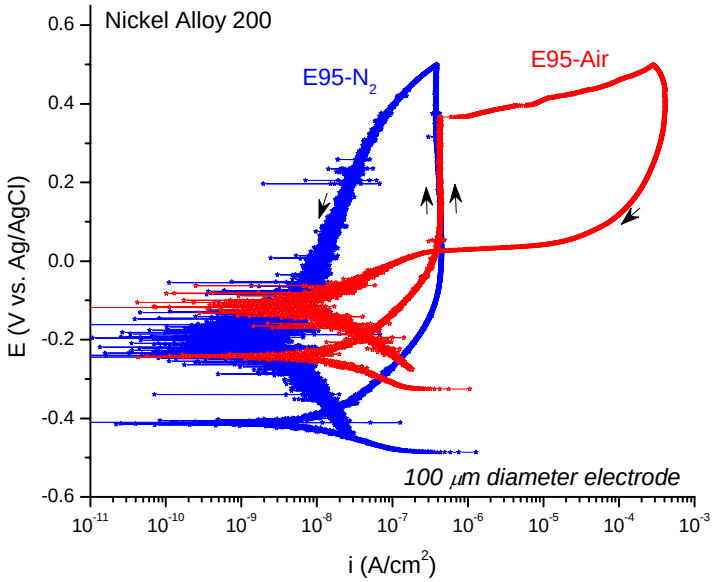

Figure 9. Comparison of CPP curves obtained for Nickel Alloy 200 in E95 at different aeration conditions.

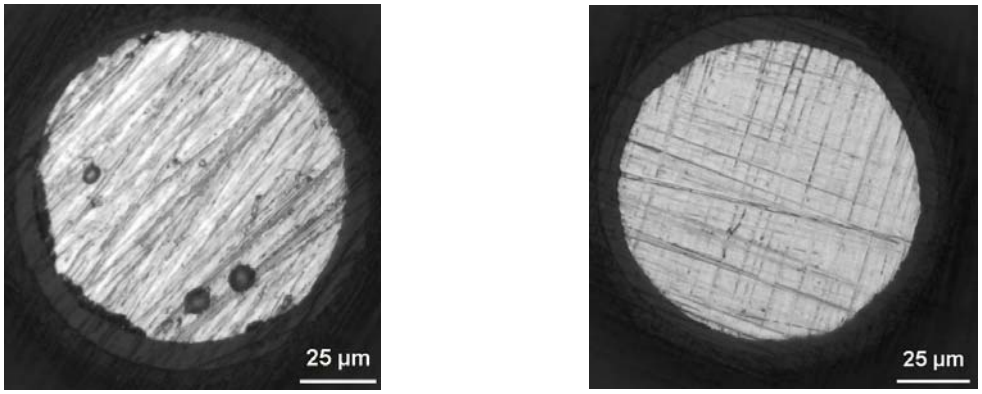

(a) (b)

Figure 10. Optical photographs of the Nickel Alloy 200 samples tested in E95 under (a) aerated condition and (b) deaerated condition.

Stainless steel 304

The CPP curves for SS304 obtained in E95 under aerated and deaerated conditions are compared in Figure 11. The curves showed negative hysteresis loop independent of purging gas, implying passive behavior in E95. No pitting corrosion was noted after the tests, as shown in Figure 12.

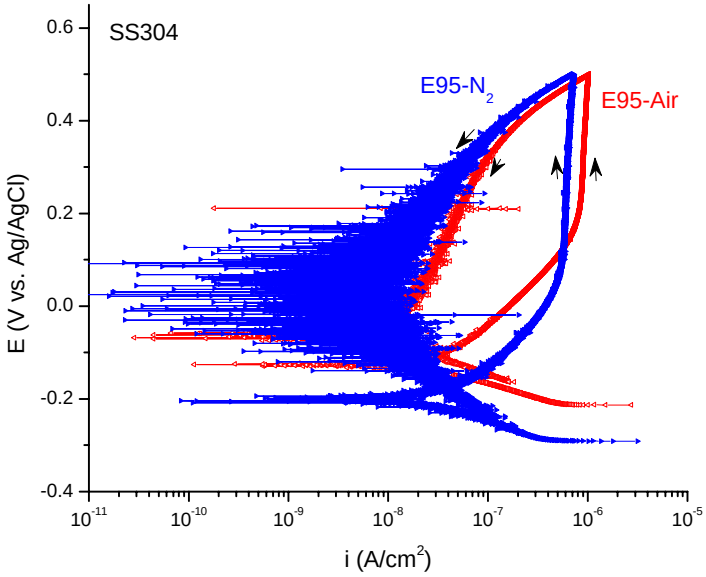

Figure 11. Comparison of CPP curves obtained for SS304 in E95 at different aeration conditions.

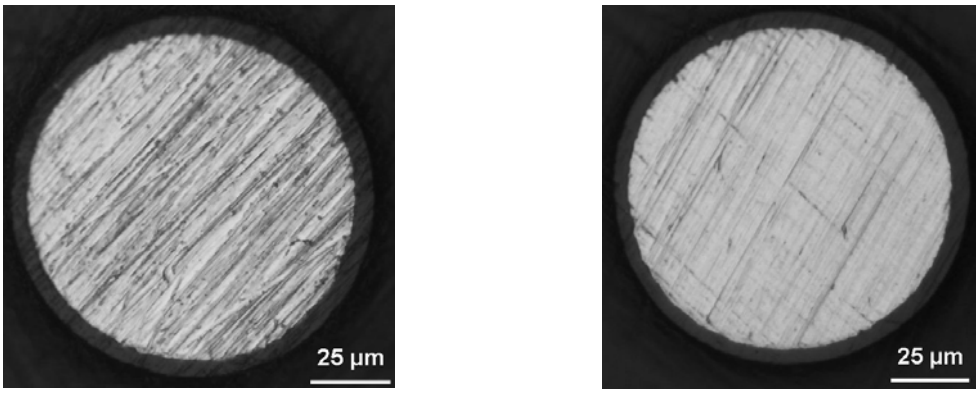

(a) (b)

Figure 12. Optical photographs of the SS304 samples tested in E95 under (a) aerated condition and (b) deaerated condition.

Stainless steel 316 in E95

The CPP curves for SS316 obtained in E95 under aerated and deaerated conditions are compared in Figure 13. Similar to that was observed for SS304, the curves showed negative hysteresis loop independent of purging gas, implying passive behavior in SFGE. No pitting corrosion was noted after the tests, as shown in Figure 14.

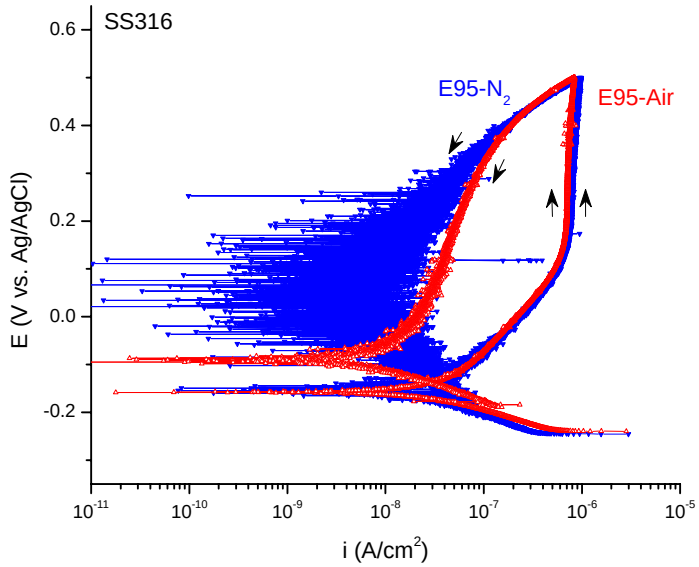

Figure 13. Comparison of CPP curves obtained for SS316 in E95 at different aeration conditions.

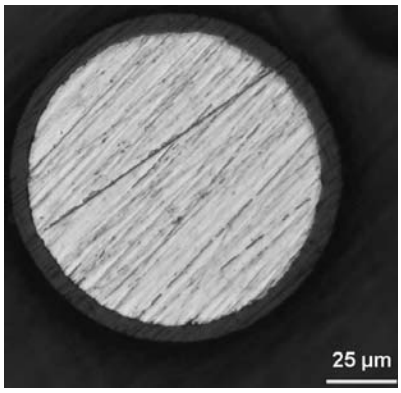

(a)

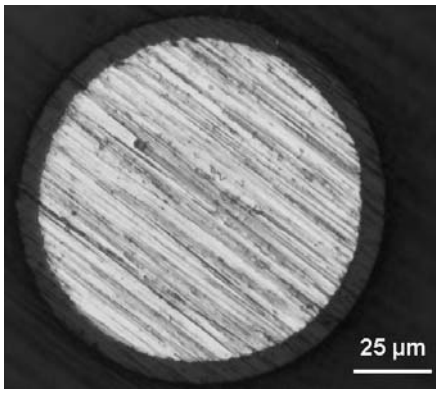

(b)

Figure 14. Optical photographs of the SS316 samples tested in E95 under (a) aerated condition and (b) deaerated condition.

Comparison of Materials Performances in E95

The OCP, pitting potential and the repassivation potential obtained in the CPP tests for different tested materials in E95 are compared in Table 5 and Figure 15. The materials susceptible to pitting corrosion were the ones with pitting potential shown in Figure 15. That is, if no pitting potential is shown in Figure 15, this indicates pitting corrosion was not observed in the CPP tests. Thus, only a few tested materials were susceptible to pitting corrosion in CPP tests. These materials are: AA7075, Bronze and Nickel alloy 200 under aerated conditions and AA7075 under deaerated conditions. It should be noted that the observation of pitting corrosion in the CPP tests does not mean that pitting corrosion would occur in the field. Rather, it only suggests that pitting corrosion could occur if the OCP was drifted above the measured pitting potentials due to certain changes. Thus, large difference between the pitting potential and the OCP generally is beneficial for the materials in terms of resistance to pitting corrosion. For the materials tested in this project, the difference between the pitting potential and the OCP is considerable and typically larger than 300 mV. However, the repassivation potential is closer to the OCP for bronze and below the OCP for AA7075, implying pitting corrosion is possible especially for AA7075 in aerated solutions.

Table 5. OCP and critical pitting potential (E_{Pit}) and repassivation potential (E_{rp}) for the materials tested in E95
(unit: V vs. Ag/AgCl).

Materials	**Aerated solution**			**Deaerated solution**		
	OCP	**E_{Pit}**	**E_{rp}**	**OCP**	**E_{Pit}**	**E_{rp}**
Aluminum 7075	-0.625	-0.031	-0.7	-0.834	-0.141	-0.7
Brass (70-30)	-0.244	-	-	-0.294	-	-
Bronze (90-10)	-0.096	0.2	0	-0.193	-	-
Nickel 200	-0.245	0.367	0	-0.410	-	-
Stainless Steel 304	-0.126	-	-	-0.204	-	-
Stainless Steel 316	-0.158	-	-	-0.154	-	-

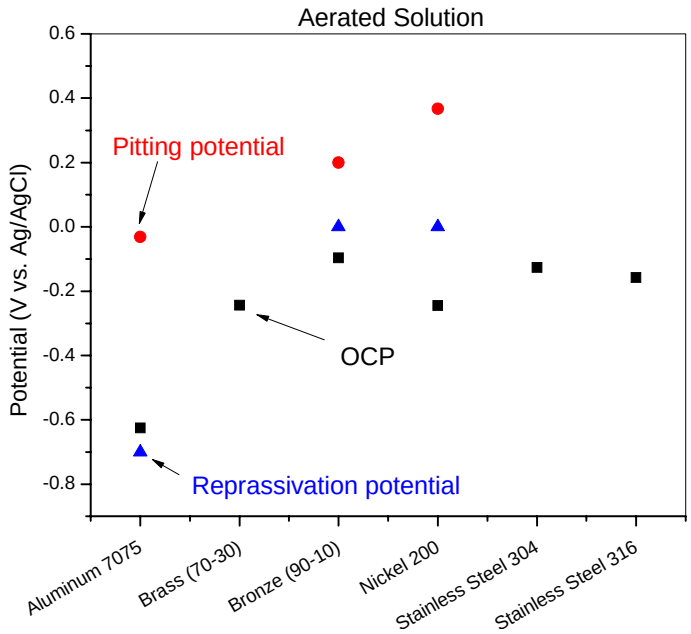

(a)

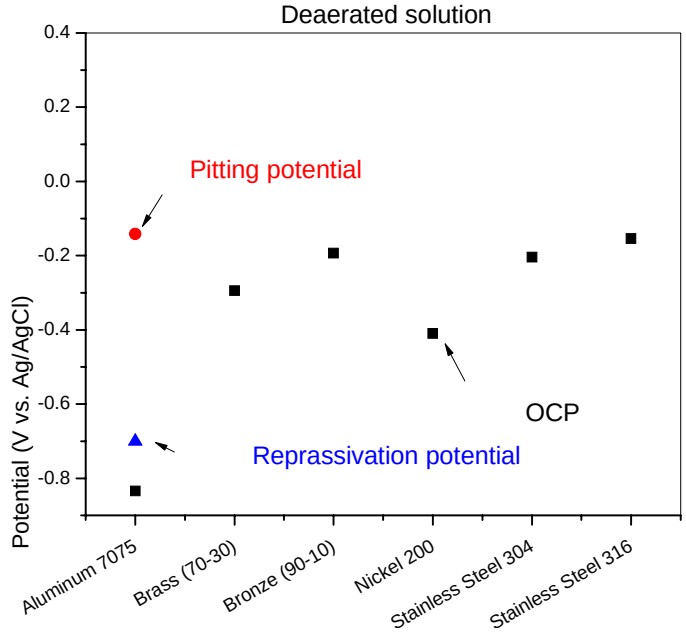

(b)

Figure 15. Comparison of the OCP, pitting potential and the repassivation potential for different tested materials in SFGE under deaerated aerated conditions (a) and deaerated conditions (b).

The corrosion rates of the tested materials in E95 under aerated and deaerated conditions are compared in Table 6 and Figure 16. As shown, the corrosion rates of most tested materials in E95 were minimal (smaller than 0.2 mpy) independent of purging gas. The only exception is bronze that showed relatively high corrosion rate, especially in aerated solution in which the bronze showed a corrosion rate of 0.8 mpy.

Table 6. Corrosion rates (mpy) of the materials tested in E95.

Materials	N_2	Air
Aluminum 7075	0.013	0.019
Brass (70-30)	0.015	0.062
Bronze (90-10)	0.417	0.8
Nickel 200	0.007	0.012
Stainless Steel 304	0.02	0.017
Stainless Steel 316	0.018	0.019

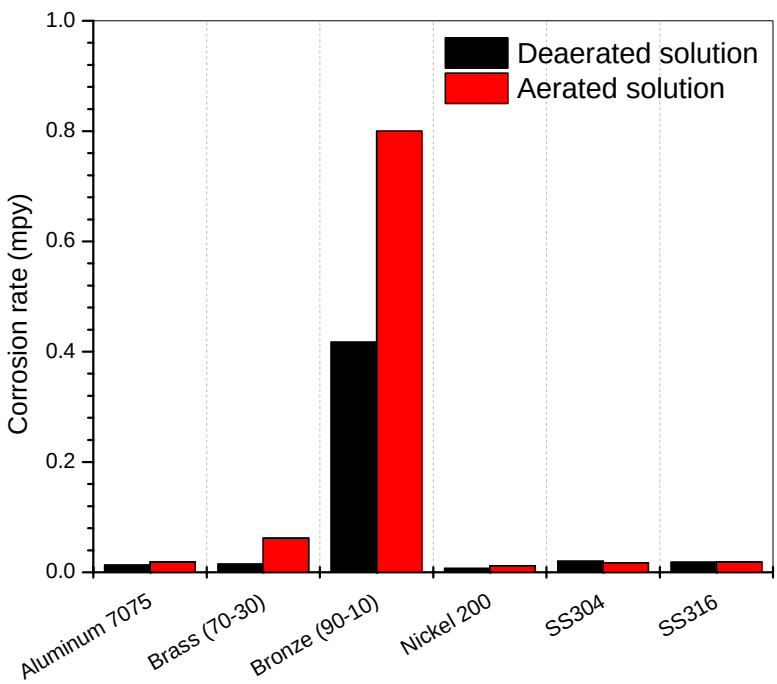

Figure 16. Comparison of the corrosion rates of the tested materials in SFGE.

3.2.3 Results in E50

In the previous research funded by PHMSA, it was found that carbon steel was more susceptible to SCC in E50 than in E95. Thus, a sub set of the materials tested in E95 was evaluated in E50 with respect to their susceptibility to pitting corrosion and general corrosion.

Aluminum 7075

The CPP curves obtained for AA7075 in E50 at different aeration conditions are compared in Figure 17. Similar to what was observed in E95, pitting corrosion was observed independent of purging gas. The pitting potential in aerated E50 was slightly higher than that in deaerated E50. In both conditions, however, the pitting potentials were lower that that obtained in E95. The corrosion attack is very clear in E50, as shown in Figure 18. The repassivation potentials for AA7075 are not very dependent of the purging gas and are approximately -0.55 V vs. Ag/AgCl, at least 250 mV more positive than the OCP.

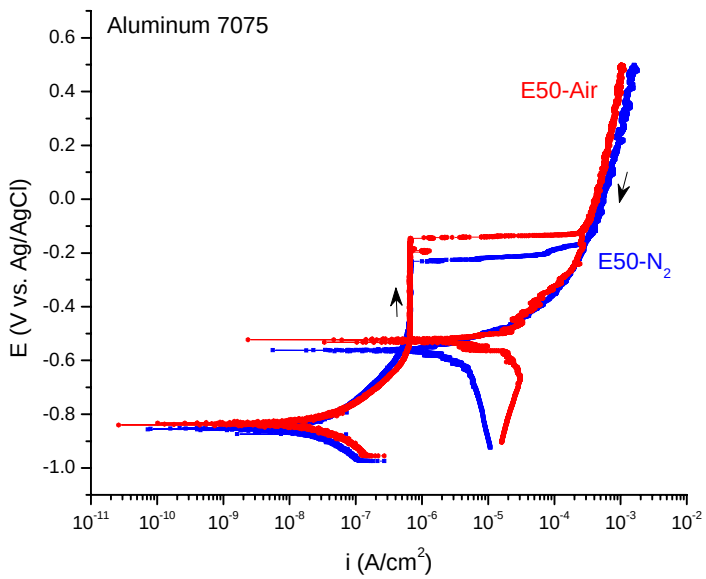

Figure 17. Comparison of CPP curves obtained for AA7075 in E50 at different aeration conditions.

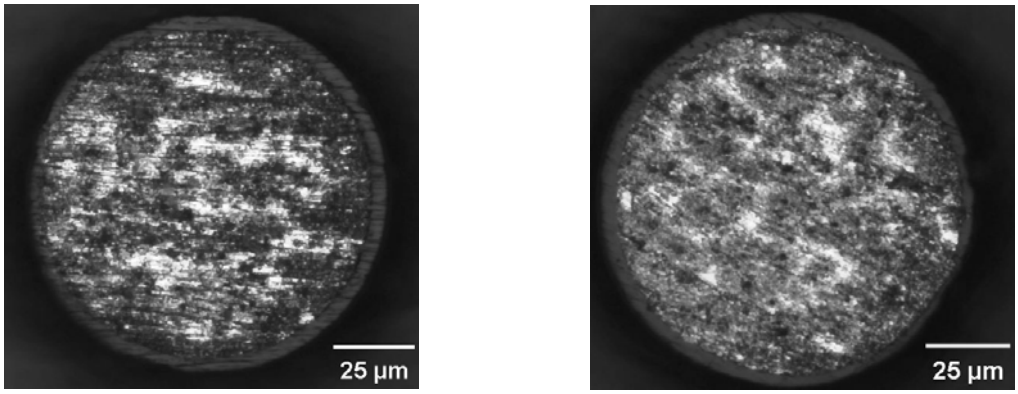

(a) (b)

Figure 18. Optical photographs of the AA7075 samples tested in E50 under (a) aerated condition and (b) deaerated condition.

Bronze 10%

The CPP curves obtained for Bronze in E50 at different aeration conditions are compared in Figure 19. The difference in the CPP curves obtained in E50 with and without oxygen is clear. In the absence of oxygen, the CPP curve showed a small hysteresis loop whereas the CPP curve showed negative hysteresis loop in the presence of oxygen. The measured current density is also much smaller when the solution was purged with air. Corrosion attack was only seen on the sample tested in deaerated E50.

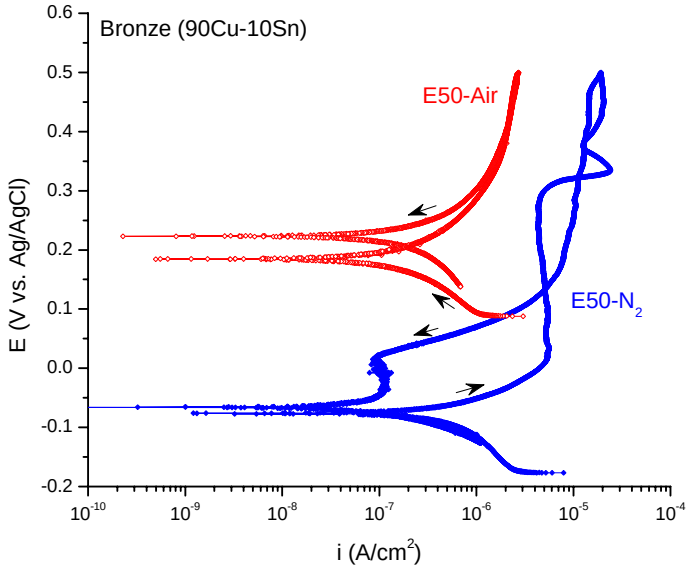

Figure 19. Comparison of CPP curves obtained for Bronze in E50 at different aeration conditions.

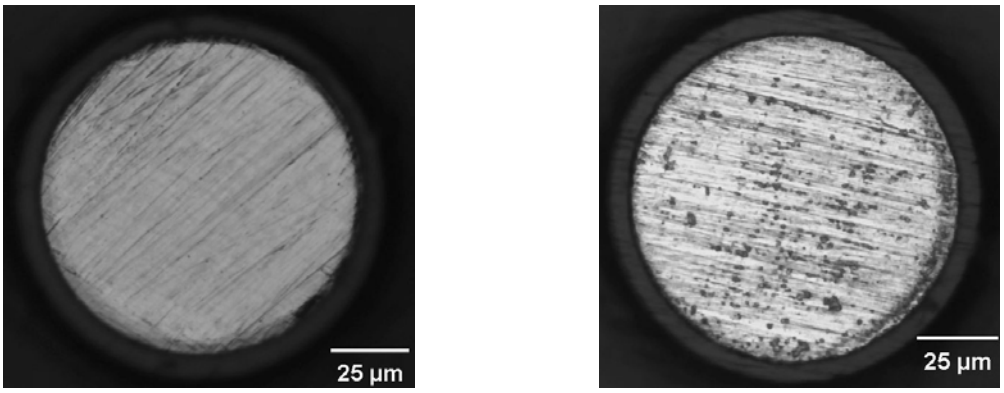

(a) (b)

Figure 20. Optical photographs of the Bronze samples tested in E50 under (a) aerated condition and (b) deaerated condition.

Nickel alloy 200

The CPP curves obtained for Nickel Alloy 200 in E50 at different aeration conditions are compared in Figure 21. Pitting corrosion was noted on the sample tested in deaerated E50 solution although the corrosion attack was very minimal (Figure 22).

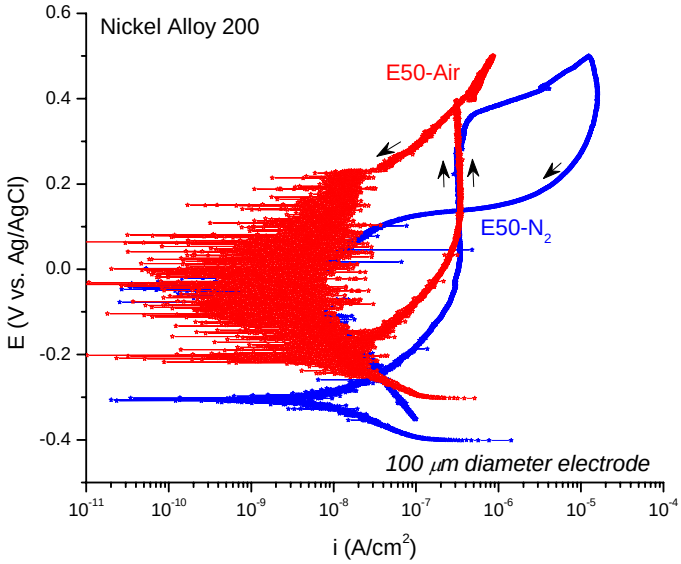

Figure 21. Comparison of CPP curves obtained for Nickel Alloy 200 in E50 at different aeration conditions.

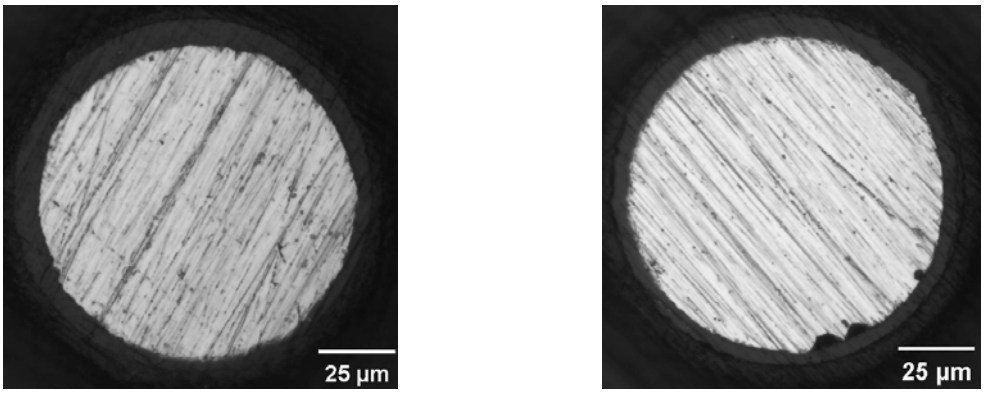

(a) (b)

Figure 22. Optical photographs of the Nickel Alloy 200 samples tested in E50 under (a) aerated condition and (b) deaerated condition.

Stainless steel 316

The CPP curves obtained for SS316 in E50 at different aeration conditions are compared in Figure 23. Stainless steel 316 remained passive in E50 solution during polarization up to +0.5 V (vs. Ag/AgCl) independent of the purging gas. No attack was noted on the tested sample and only a few surface stains were observed (Figure 24).

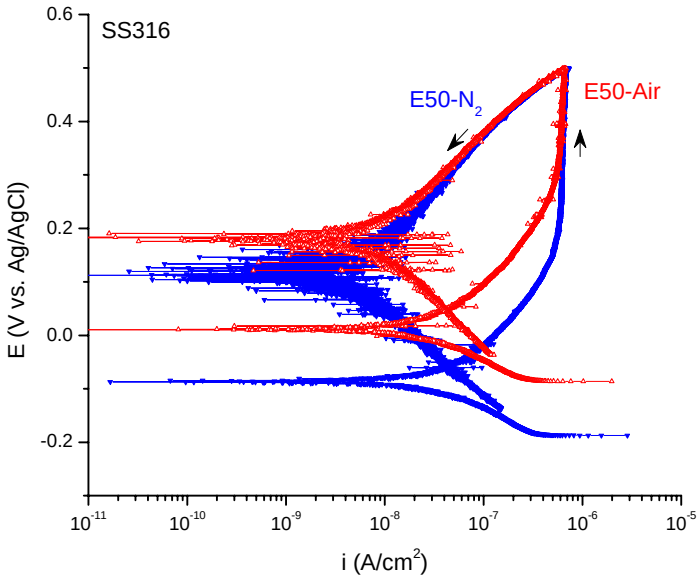

Figure 23. Comparison of CPP curves obtained for Nickel Alloy 200 in E50 at different aeration conditions.

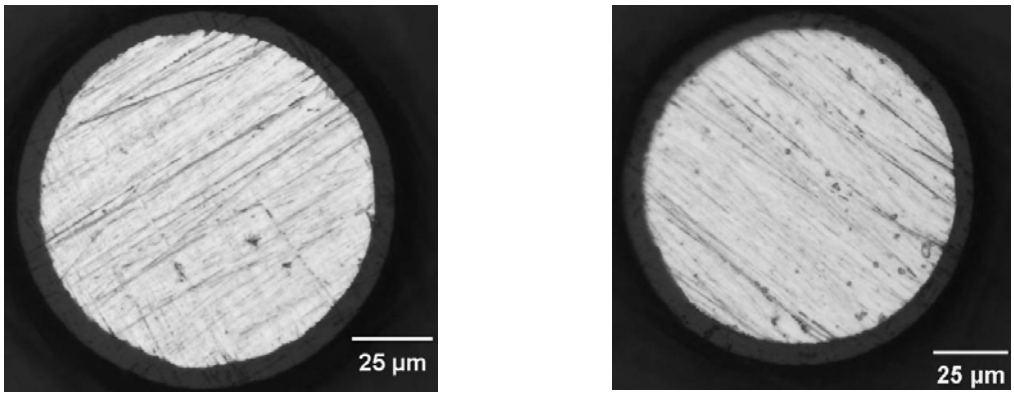

(a) (b)

Figure 24. Optical photographs of the Nickel Alloy 200 samples tested in E50 under (a) aerated condition and (b) deaerated condition

Comparison of Materials Performances in E50

The OCP and pitting potential and the corrosion for the tested materials in E50 under aerated and deaerated conditions are compared in Table 7 and Figure 25. Note that the material was found to be susceptible to pitting corrosion if pitting corrosion is shown in the figure. Similar to that was observed in E95, the materials were more susceptible to pitting corrosion in deaerated solutions compared to aerated conditions. However, in the cases where pitting corrosion was observed, the difference between the repassivation potential and the OCP is always greater than 250 mV, meaning that pitting corrosion was observed but a large safety margin (the difference between OCP and pitting potential) exists.

Table 7. Comparison of OCP, critical pitting potential (E_{Pit}) and the repassivation potential (E_{rp}) for the materials tested in E50 (unit: V vs. Ag/AgCl).

Materials	**Aerated solution**			**Deaerated solution**		
	OCP	**E_{Pit}**	**E_{rp}**	**OCP**	**E_{Pit}**	**E_{rp}**
Aluminum 7075	-0.840	-0.146	-0.5	-0.856	-0.234	-0.55
Bronze (90-10)	0.184	-	-	-0.076	0.280	0.1
Nickel 200	-0.201	-	-	-0.306	0.360	0.15
Stainless Steel 316	0.010	-	-	0.056	-	-

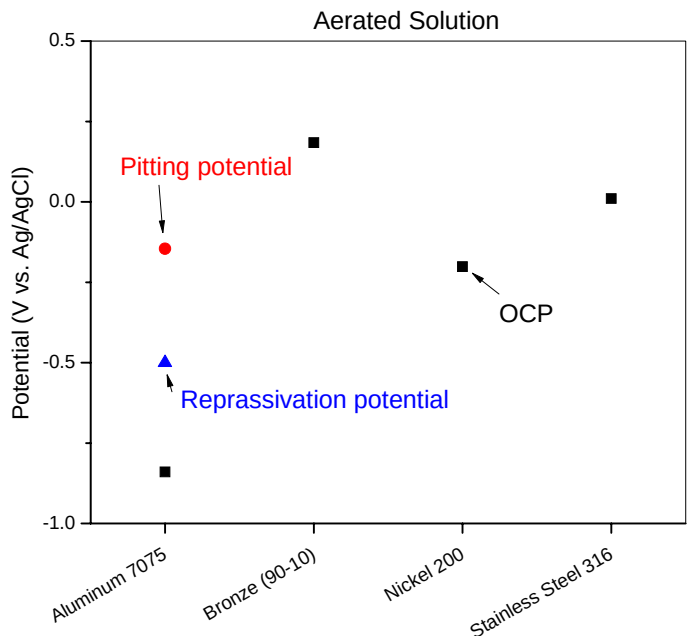

(a)

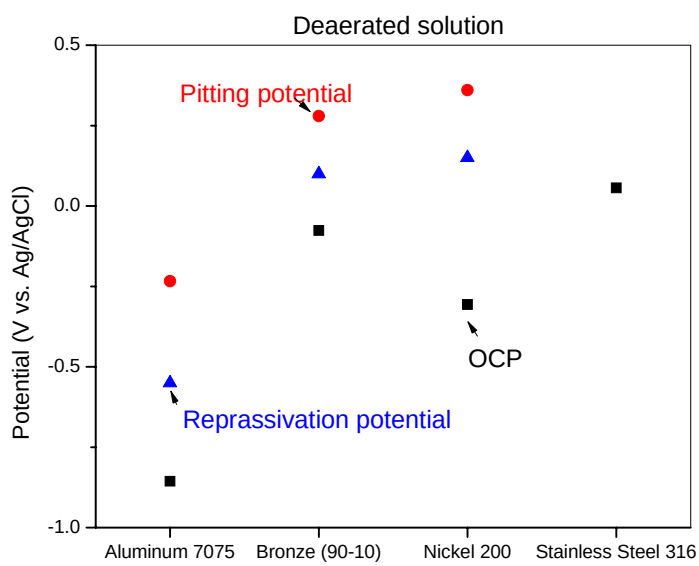

(b)

Figure 25. Comparison of OCP, pitting potential and repassivation potential for different tested materials in E50 under deaerated aerated conditions (a) and deaerated conditions (b).

The corrosion rates of the tested materials in E50 in deaerated and aerated conditions are compared in Table 8 and Figure 26. The corrosion rates are small for all tested materials except for the bronze. Similar to in E95, bronze experienced the highest corrosion rate. The corrosion rate of the Bronze in deaerated E50 is similar to that in deaerated E95 although its corrosion rate is lower in aerated E50 compared to aerated E95. In all cases, the corrosion rate was minimal with the maximum corrosion rate at 0.4 mpy (0.01 mm/y).

Table 8. Corrosion rate (mpy) of non-ferrous materials in E50

Materials	N_2	Air
Aluminum 7075	0.011	0.014
Bronze (90-10)	0.409	0.108
Nickel 200	0.006	0.008
Stainless Steel 316	0.014	0.013

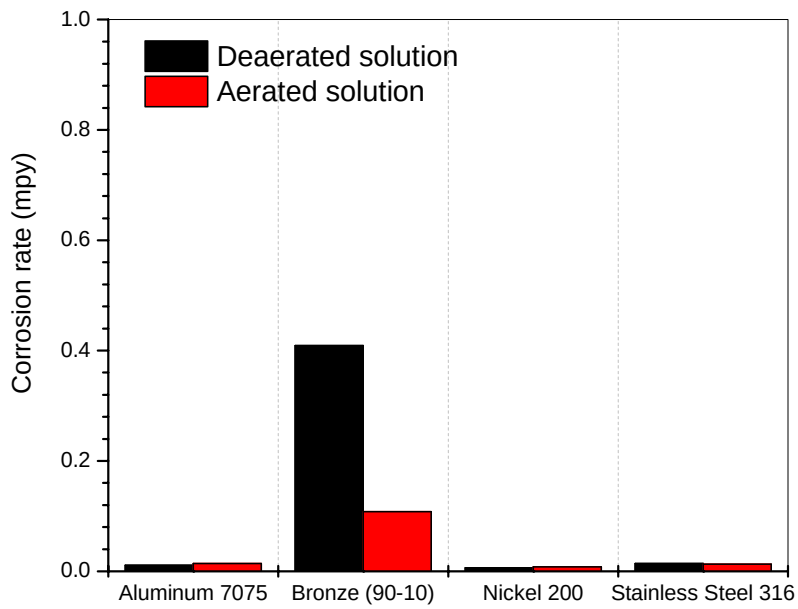

Figure 26. Comparison of corrosion rates of the tested materials in SFGE.

3.2.4 Results in E95 with 37.5 ppm NH_4OH

It was found in a previous research funded by PHMSA that SCC of carbon steel in FGE can be effectively mitigated by adding 37.5 ppm NH_4OH. The addition of NH_4OH would increase the pH of the FGE but also will introduce ammonia into the solution. Thus, it is essential to develop some knowledge about the compatibility of the non-ferrous materials with FGE in the presence of NH_4OH. It should be pointed out that it is not the objective of this work to investigate whether NH_4OH can inhibit corrosion of the tested materials. Rather, the investigation was focused on whether the addition of NH_4OH would increase the corrosion rate of the materials in E95. Tests

were only performed in deaerated conditions since most materials showed pitting corrosion in the CPP tests in deaerated E95, as discussed above.

Three materials were evaluated: AA7075, Bronze and Nickel Alloy 200. The CPP curves were compared to the results obtained for the same materials in E95 without NH_4OH added. The pitting potential of AA7075 was moved to ~-175 mV vs. Ag/AgCl to 250 mV vs. Ag/AgCl after adding NH_4OH, as shown in Figure 27. So NH_4OH appeared to be able to provide some inhibition on the pitting corrosion of AA7075 in E95. For Bronze, however, the addition of NH_4OH increased the measured current (Figure 29) and the corrosion of Nickel Alloy 200 was not changed by 37.5 ppm NH_4OH (Figure 31).

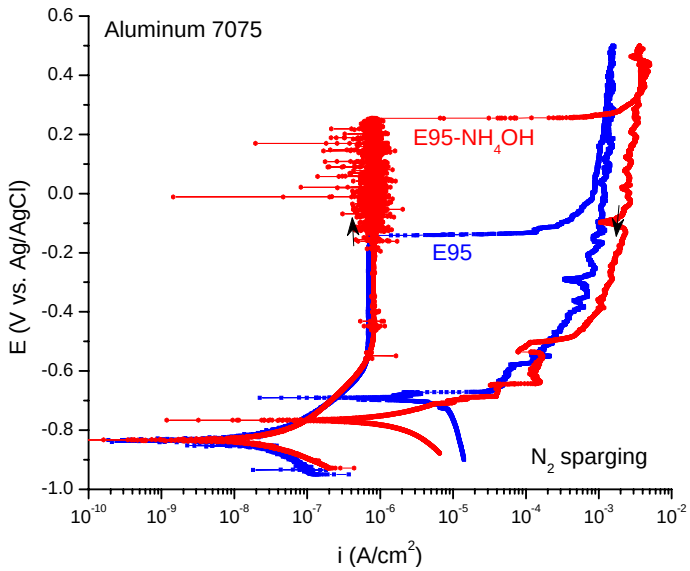

Figure 27. Comparison of CPP curves obtained for AA7075 in deaerated E95 with 37.5 ppm NH_4OH.

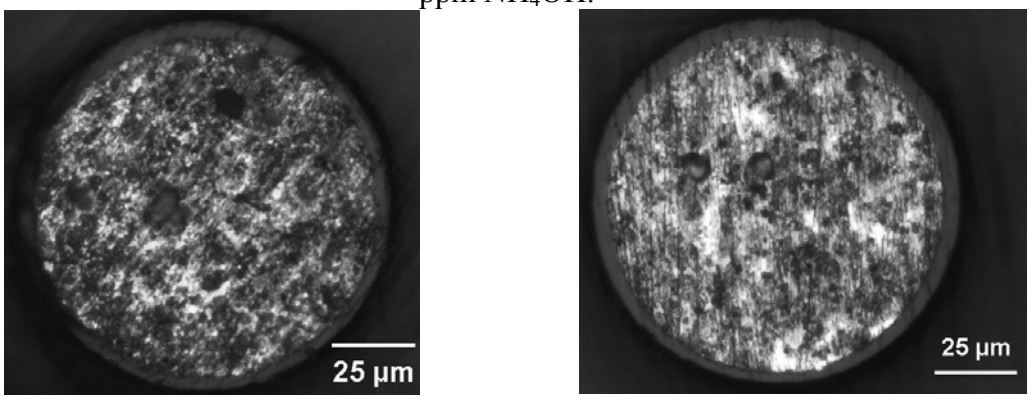

(a) (b)

Figure 28. Optical photographs of the AA7075 samples tested in deaerated E50. (a) with 37.5 ppm NH_4OH; (b) without NH_4OH.

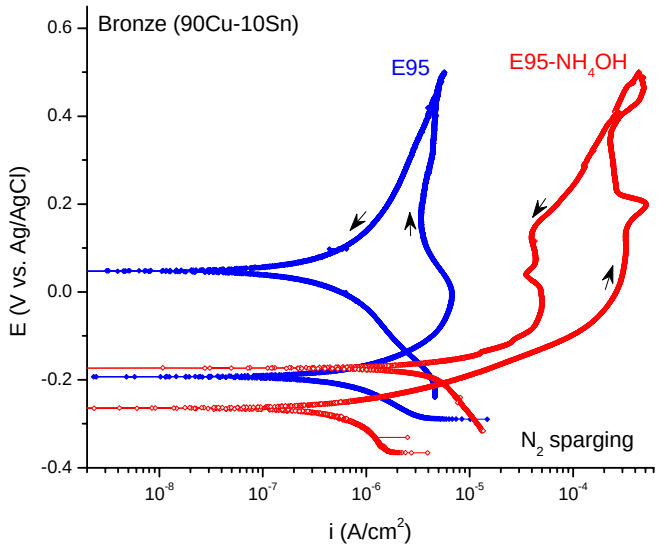

Figure 29. Comparison of CPP curves obtained for Bronze in deaerated E95 with 37.5 ppm NH_4OH.

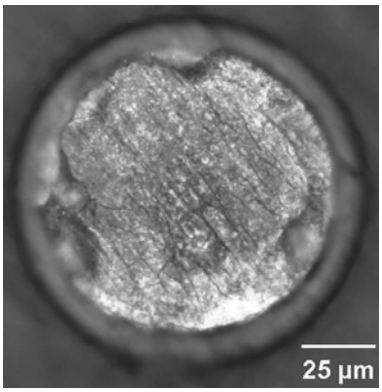

(a)

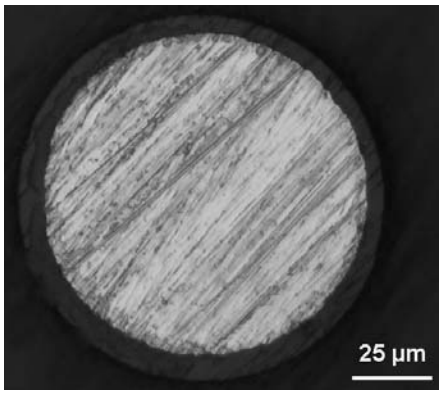

(b)

Figure 30. Optical photographs of the Bronze samples tested in deaerated E50. (a) with 37.5 ppm NH_4OH; (b) without NH_4OH.

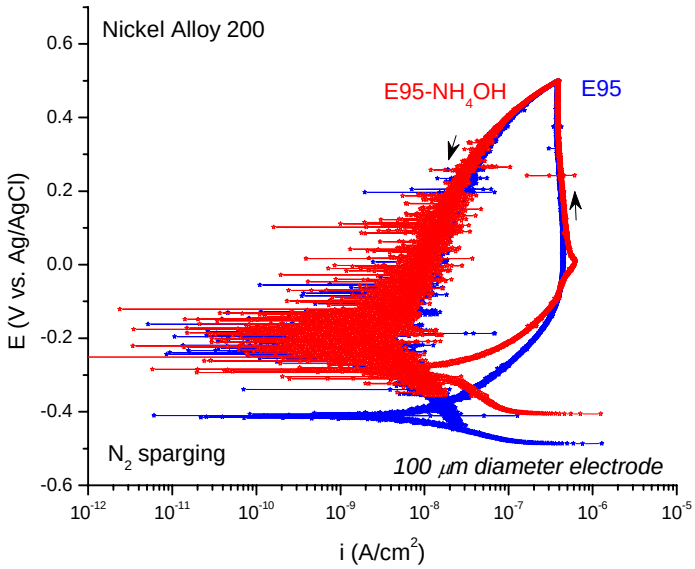

Figure 31. Comparison of CPP curves obtained for Nickel Alloy 200 in deaerated E95 with 37.5 ppm NH_4OH.

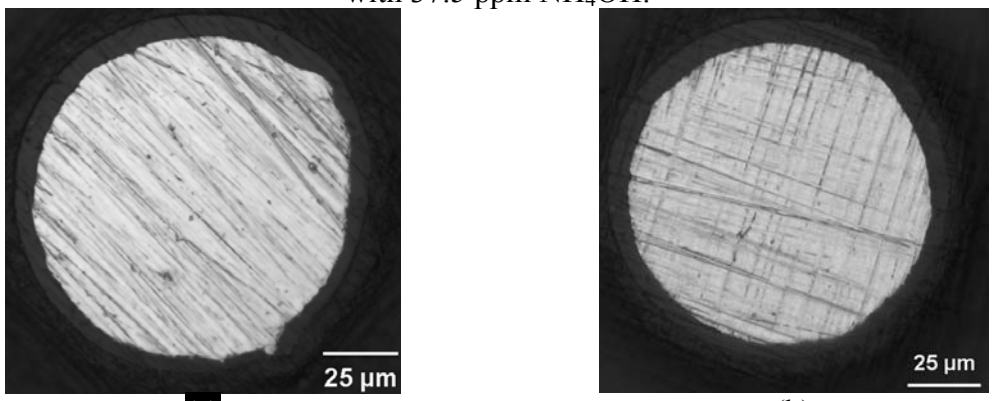

(a) (b)

Figure 32. Optical photographs of the Nickel Alloy 200 samples tested in deaerated E50. (a) with 37.5 ppm NH_4OH; (b) without NH_4OH.

<u>Comparison of Materials Performances in Deaerated E95 with 37.5 ppm NH_4OH</u>

The corrosion rates of the tested materials are compared in Table 9 and Figure 33. As shown, the corrosion rates of AA7075 and Nickel alloy in deaerated E95 with 37.5 ppm NH_4OH are very small. Similar to that observed in all other solutions, bronze showed the highest corrosion rate—albeit still small (~0.4 mpy).

Table 9. Corrosion rate (mpy) of non-ferrous materials in deaerated E95 with 37.5 ppm NH_4OH.

Materials	E95	E95+NH_4OH
Aluminum 7075	0.013	0.017
Bronze (90-10)	0.417	0.453
Nickel 200	0.007	0.011

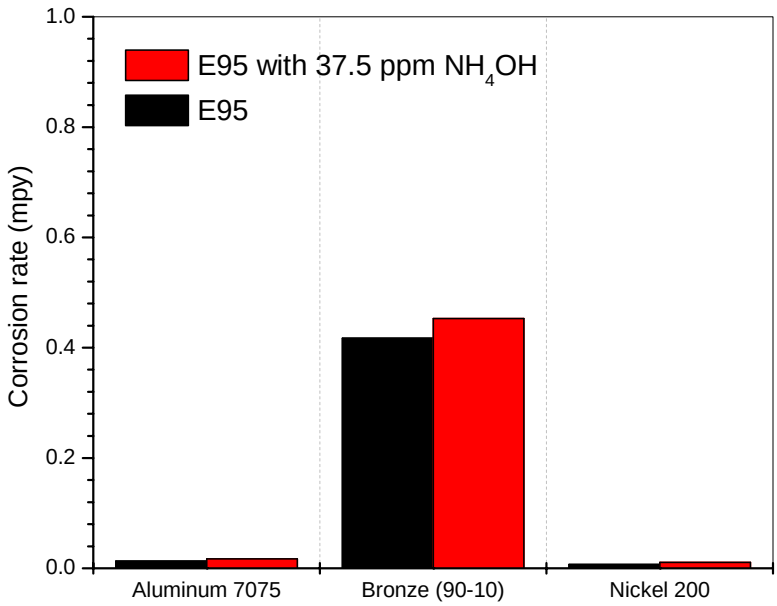

Figure 33. Comparison of corrosion rates of the tested materials in deaerated E95 with and without 37.5 ppm NH_4OH.

4.0 GENERAL DISCUSSION

The tested materials showed minimal general corrosion rate, even for Bronze 10% which had the highest corrosion rates in the tests compared to other materials independent of solutions. Pitting corrosion was observed on several materials: AA7075, Bronze 10%, and Nickel Alloy 200. In some cases where pitting corrosion was observed, such as AA7075 in aerated E95, the repassivation potential was below OCP, indicating pitting could occur giving enough exposure time. In other cases, the repassivation was considerable more positive than the OCP and thus pitting corrosion is less likely. No substantial difference was noted between the tests performed in E50 and E95 although carbon steel was found to be more prone to SCC in E50 in prior research. The addition of 37.5 ppm NH_4OH as an inhibitor slightly increased the measured

corrosion rate on the Bronze sample but did not change the corrosion performance of other two tested materials. These results obtained from the laboratory tests imply that the tested materials are most likely compatible with FGE with the exception of AA7075 and Bronze. However, it needs to be noted that the long term performance of the materials in FGE was not addressed in the tests. This aspect is particularly important for the materials susceptible to pitting corrosion but with the repassivation potential below (e.g., AA7075) or close to the OCP. The OCP shift over time needs to be investigated to determine how fast the repassivation potential can be reached. Additionally, the corrosion rate obtained in a long term evaluation would be more representative of the corrosion rate experienced by the materials in the field.

5.0 SUMMARY

- AA7075, Bronze 10% and Nickel Alloy were found to be susceptible to pitting corrosion in the laboratory tests. AA7075 had a repassivation potential below the open circuit potential (OCP) in aerated E95, indicating a high likelihood of pitting corrosion. Bronze 10% also had a repassivation close to the OCP in the aerated E95, meaning the likelihood of pitting corrosion is higher than other tested materials.

- The materials did not show a substantial difference in the corrosion performance in E50 and E95.

- The general corrosion rates, in general, were very low for all materials in all tested solutions.

- The general corrosion rate of Bronze 10% was the highest among all tested materials independent of tested solutions and the purging gas but was low from the standpoint of material integrity.

- The addition of 37.5 ppm NH_4OH did not substantially alter the material corrosion performance of the tested materials. An increase in the anodic current was noted for Bronze 10% in E95 in the presence of 37.5 ppm NH_4OH but the corrosion rate was still minimal.

6.0 REFERENCES

1. Evans, U. R., Metallic Corrosion, Passivity, and Protection, Longmans, Green, and Co., New York, NY, 1948.

2. Gindin, L. G., Ambarzumian, R. S., and Belchikova, E. P., Comptes, rend. Dolk. Acad. Sci. U.R.S.S., Vol. 29, No. 44. 1940.

3. Bushrod, C. J., Met. Ind., Volume 61, 1942.

4. R, D. Kane, D. Eden, N. Sridhar, J. Maldonado, M.P.H. Brongers, A. K. Agrawal, and J. A. Beavers, "Stress Corrosion Cracking of Carbon Steel in Fuel-Grade Ethanol: Review, Experience Survey, Field Monitoring, and Laboratory Testing," API Technical Report 939-D, Second Edition, May 2007.

5. Roques, et al., "Stress Corrosion Cracking and Pitting Corrosion Relation for Zircaloy-4 in Chloride Containing Hydro-Alcoholic Media," Electrochimica Acta, Volume 32, No. 6, 1987.

6. Singh, V. B., and Singh, V. K., "Corrosion Behavior of Stainless Steel (AISI 321) in Alcoholic-H2SO4 Mixtures," Materials-Transactions, JIM. Volume 32, No. 3, 1991.

7. Renewable Fuel Association Publication #96051, Fuel Ethanol, Industry Guideline, Specification, and Procedure, December 2003.

8. Gregory T. Quickel, John A. Beavers, "Determining the Effects of Ethanol on Pump Station Facilities", PRCI Report PR-186-09204, PRCI, April 2010.

9. Feng Gui, J. A. Beavers, and Narasi Sridhar, "Evaluation of Ammonia Hydroxide for Mitigating Stress Corrosion Cracking of Carbon Steel in Fuel Grade Ethanol", Paper# 11138, Corrosion 2011 (NACE International).

10. F. Gui**,** N. Sridhar, "Method for Conducting Electrochemical Experiments in Resistive Environments", *Corrosion,* 66*,* 045005(2010).

11. ASTM D 4806-01a 2001, "Standard Specification for Denatured Fuel Ethanol for Blending with Gasoline for Uses with Automotive Spark-ignition Engine Fuel" (West Conshohocken, PA: ASTM International, 2001).

12. C. Amatore, M. R. Deakin and R. M. Wightman, *Journal of Electroanalytical Chemistry*, 225, 49 (1987).

Det Norske Veritas

Det Norske Veritas (DNV) is a leading, independent provider of services for managing risk with a global presence and a network of 300 offices in 100 different countries. DNV's objective is to safeguard life, property and the environment.

DNV assists its customers in managing risk by providing three categories of service: classification, certification, and consultancy. Since establishment as an independent foundation in 1864, DNV has become an internationally recognized provider of technical and managerial consultancy services and one of the world's leading classification societies. This means continuously developing new approaches to health, safety, quality and environmental management, so businesses can run smoothly in a world full of surprises.

Global Impact for a Safe and Sustainable Future

Learn more on www.dnv.com